Molecular Crystals and Liquid Crystals Science and Technology. Section A. Molecular Crystals and Liquid Crystals
Publication details, including instructions for authors and subscription information:
http://www.tandfonline.com/loi/gmcl19

Compared Study of a Quenched Blue Phase by Direct Transmission Electron and Atomic Force Microscopy

HÉLÈNe Dumoulin [a] , Pawel Pieranski [a] , HervÉ Delacroix [b] , Inge Erk [b] , Jean-Marc Gilli [c] & Yves Lansac [d]

[a] Laboratoire de Physique des Solides, Bât. 510, Université Paris-Sud, F-91405, Orsay, Cedex, FRANCE

[b] Centre de Génétique Moléculaire, CNRS, F-91198 Gif-sur, Yvette, Cedex, FRANCE

[c] Institut Non Linéaire de Nice, CNRS UMR 129, Sophia Antipolis, F-06560, Valbonne, FRANCE

[d] Laboratoire de Physique de la Matière Condensée, URA 190, Parc Valrose, F-06108, Nice, FRANCE

Version of record first published: 23 Sep 2006.

To cite this article: HÉLÈNe Dumoulin , Pawel Pieranski , HervÉ Delacroix , Inge Erk , Jean-Marc Gilli & Yves Lansac (1995): Compared Study of a Quenched Blue Phase by Direct Transmission Electron and Atomic Force Microscopy, Molecular Crystals and Liquid Crystals Science and Technology. Section A. Molecular Crystals and Liquid Crystals, 262:1, 221-233

To link to this article: http://dx.doi.org/10.1080/10587259508033527

Mol. Cryst. Liq. Cryst. 1995, Vol. 262, pp. 221–233
Reprints available directly from the publisher
Photocopying permitted by license only

COMPARED STUDY OF A QUENCHED BLUE PHASE BY DIRECT TRANSMISSION ELECTRON AND ATOMIC FORCE MICROSCOPY

HÉLÈNE DUMOULIN*, PAWEL PIERANSKI*, HERVÉ DELACROIX**, INGE ERK**, JEAN-MARC GILLI***, YVES LANSAC****

* Laboratoire de Physique des Solides, Bât. 510, Université Paris-Sud, F-91405 Orsay Cedex, FRANCE

** Centre de Génétique Moléculaire, CNRS, F-91198 Gif-sur-Yvette Cedex, FRANCE

*** Institut Non Linéaire de Nice, CNRS UMR 129, Sophia Antipolis, F-06560 Valbonne, FRANCE

**** Laboratoire de Physique de la Matière Condensée, URA 190, Parc Valrose, F-06108 Nice, FRANCE

Abstract A side chain mesomorphic cooligomer presents a large blue phase temperature domain. The cooling down of the sample from BPI allows to quench coloured crystallites below the glass transition of this material. Observations by transmission electron microscopy on microtome cuts of these crystallites reveal the presence of mono- and bi-periodic domains corresponding to the respective quench of cholesteric and BPI phases at room temperature. The use of an atomic force microscopy technique directly on the cuts observed by electron microscopy, and the detection of the same textures by both methods reveal unambiguously that the TEM contrast originates from strong, "cut-induced", surface relief. The nature of this corrugation is discussed using numerical simulations derived from a Ginzburg-Landau approach.

INTRODUCTION

The use of polymeric or oligomeric cholesteric materials possessing a glass transition above room temperature allows to quench the liquid crystal Ch* or BPI phases[1]. It is consequently possible to obtain thin (≈ 70 nm) microtome cuts of these quenched samples and to observe directly, by low enlargement TEM technique[2], the periodic textures associated to these phases. The photomicrographs of Fig. 4, 6a and 7a give some examples of the images obtained. These observations rose the question of the origin of the contrast

in such images. As developed in ref.(3), the observation of the dislocations in the Ch* periodic domains as well as the results obtained by a sophisticated image analysis technique on the BPI domains strongly suggest that this contrast could account for the orientational order parameter in the bulk of the cut and not for a surface deformation associated to this cut, as encountered in the extensively used freeze fracture and metal replica techniques.

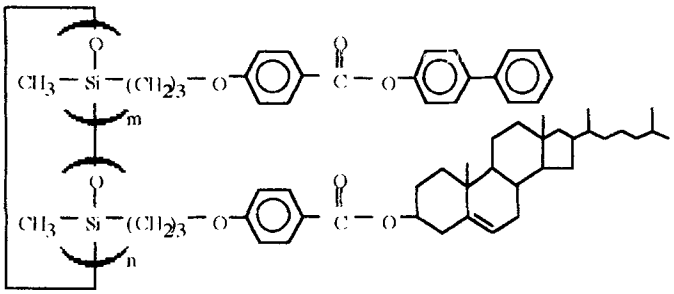

FIGURE 1 Formula of the material used. $3 \leq n+m \leq 7$.

The aims of the present work are (1°) to examine by an AFM technique the topography of the same cuts that have been used in the previous TEM studies and (2°) to compare this topography with the contrast of the TEM images. The feasibility of such experiments was suggested by a recent work with an atomic force microscopy (AFM) technique[4] done on a quenched free surface of the Cholesteric phase of the same oligomer. Indeed, this study showed the adequacy of the AFM method to analyse easily the surface topography of this material.

EXPERIMENTAL

The considered industrial oligomer is described in ref.(1); its formula is given in Fig. 1. The oligomer samples sandwiched between glass plates and containing blue phase platelets were quenched by simple contact with a metallic plate at room temperature. In such samples cooled to room temperature, the glittering blue phase platelets were

preserved and directly visible with naked eye or with a polarising microscope (Fig. 2).

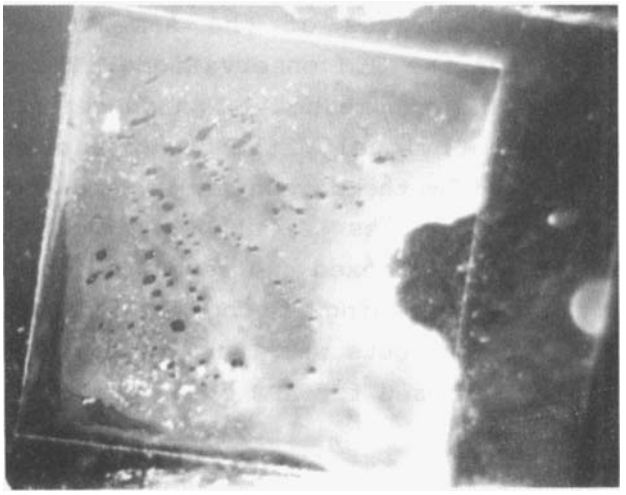

FIGURE 2 Photograph in reflecting microscope of a sample with BP crystallites. See Color Plate I.

After removal of the cover slide, the portions of the sample with BP platelets were scratched away and embedded in a resin. Subsequently, they were cut with a microtome into thin slices which were investigated with a Philips CM12 electron microscope used in transmission mode at low magnification. Fig. 3 gives a schematic representation of the microtome operation, followed by two methods of "fishing" of the floating cuts. See Color Plate I.

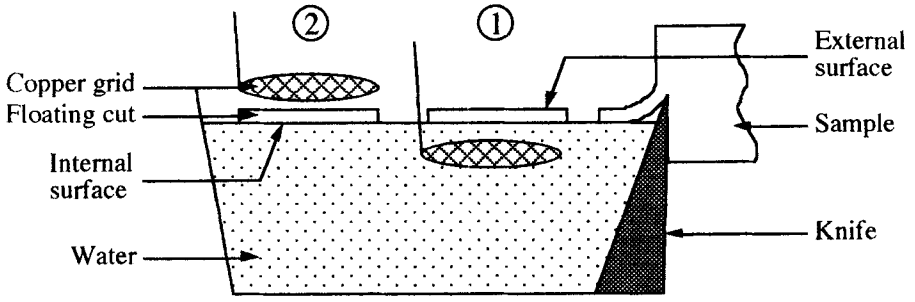

FIGURE 3 Scheme of the microtome cutting and "fishing" procedures.

The AFM observations were made with a NanoScope III (Digital Instruments) used in the tapping™ mode, which does not damage the sample surface. They were carried out directly on free surfaces of the same cuts that were previously used for the TEM observations. These cuts were deposited, by the fishing method 1, on copper grids covered with carbon films. Obviously, the lower surfaces of such cuts being supported by the carbon films were not accessible for AFM studies. New series of cuts obtained with the same samples were carefully indexed and deposited on copper grids alternating the two "fishing" methods. In the case of the fishing method "2", the cuts were turned upside down so that the lower face was exposed for AFM observations.

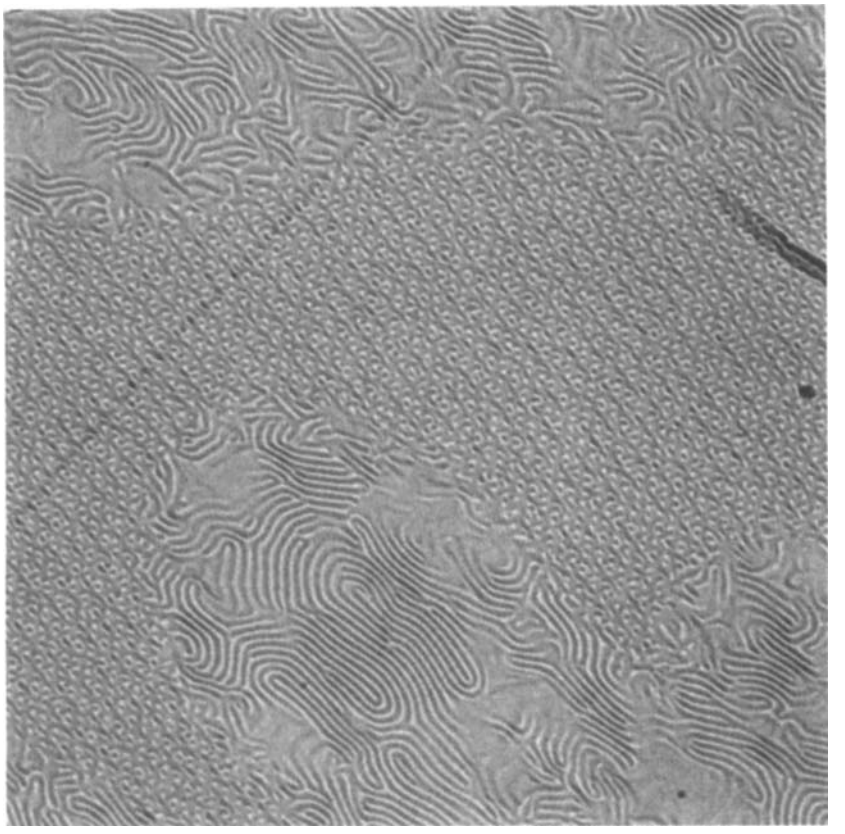

FIGURE 4 TEM positive image of BPI and Ch*.

EXPERIMENTAL RESULTS

TEM experiments

Fig. 4 shows the transmission electron microscopy image of a section of a quenched cooligomer sample. The central region of the image displays an intricate texture corresponding to a random orientation of the section through a BPI phase domain. This region is surrounded by the fingerprint texture of the cholesteric phase. The continuity of black and white contrast between the two phases is clearly visible. The straight line corresponds to the direction of the cutting knife.

To identify the observed structure and understand the aspect of the texture, as well as to throw some new light on the origin of the contrast in such systems, it was necessary to be able to index the diffraction pattern (Fig. 5).

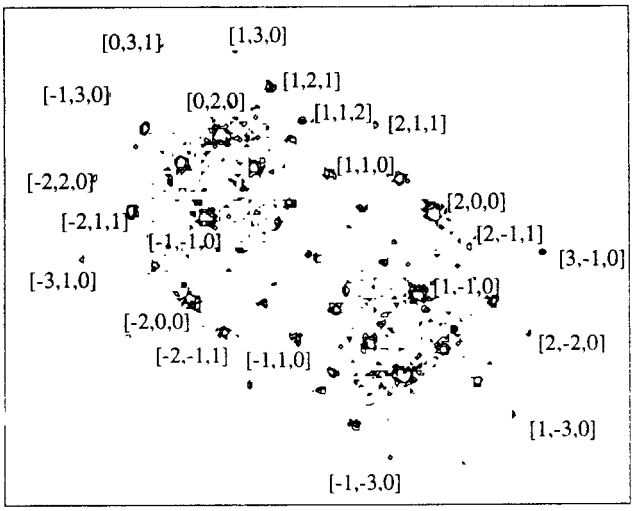

FIGURE 5 Fourier transform of a selected area in Fig. 4. (For clarity, only peripheral reflections are indexed).

As the orientation of the cut with respect to the cubic lattice is entirely random, this indexing can prove complex. Furthermore, the softness of the material, cut at room temperature, is responsible for a compression in the

direction of the cut, yielding an elongation of the diffraction pattern in the same direction. These difficulties can be avoided by the use of a model[3] defining the relationship between the 2-D Fourier transform of the image and the 3-D reciprocal space of the BP crystal.

Following this model, the diffraction pattern stretched by the cutting process was indexed by a trial-and-error procedure. The final indexing was assessed by the following remarks:

- as awaited in the O^{8-} symmetry case, the computed value of the unit cell is close to the cholesteric pitch.

- the direction of the cut-induced compression is also close to the one obtained directly from the observation of the traces of the knife.

Systematic extinctions observed on the obtained indexed pattern correspond to the selection rule: h + k + l = 2n. Reflections [110], [200], [211], [220], already detected in optical experiments on BPI of O^8 space group, are also present here.

It is of great importance to note the presence of the spots [200], as they are forbidden in the O^8 symmetry group in the general case of X-ray diffraction, i.e. for a scalar electron density order parameter. The presence of these spots suggests that TEM experiments are somehow sensitive to the director orientation.

TEM experiments with the sample tilted with respect to the electron beam have been carried out. The same area was investigated with a tilt angle varying from 0° to 55°. The pattern obtained was only shrunk in one direction, but the contrast was not qualitatively modified by the tilt (It would have been altered in the case of bulk scattering contrast).

AFM experiments

Due to their intrinsic elasticity, the samples supported by the copper grids posses some vibration eigenmodes which frequencies are defined, among other parameters, by the

geometry of the grid holes. Some of these eigenmodes were excited by the cantilever when operating in the tapping mode.

Fortunately, the efficiency of the coupling was weak enough in the vicinity of the hole borders, so that AFM images free of parasitic effects, such as these in figs 6b and 7b, could be recorded from some sample areas much smaller then the grid holes. After a careful comparison of these images with the previously recorded TEM image of the whole hole, the corresponding areas have been identified. They are shown in figs. 6a and 7a.

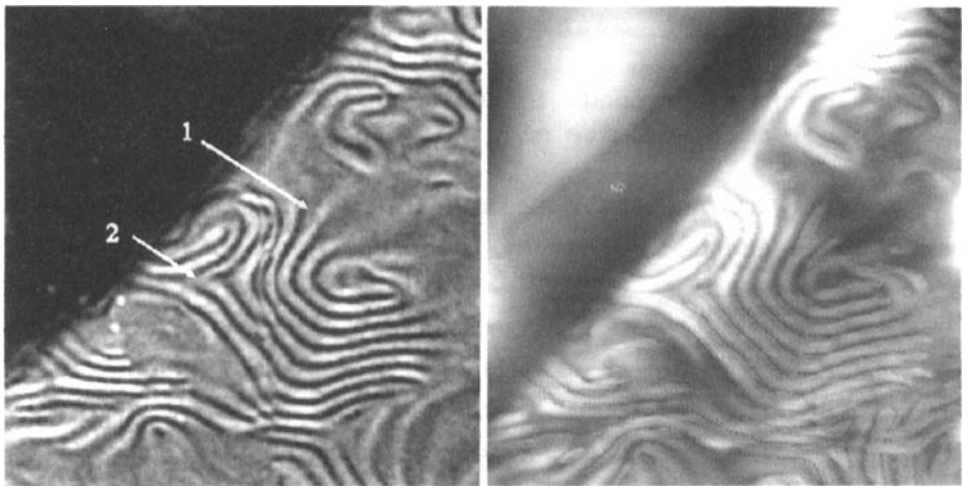

FIGURE 6 a) TEM image (negative); b) AFM image of the same area. The size is 5 μm $\times$ 5 μm.

It is important to emphasise here that the substantial relief ($\approx$ 20 nm) generating the AFM contrast obtained here is observed only on the "external" side of the cut (Fig. 3). When the second type of fishing technique (capillary adhesion) is used, the TEM contrast remains the same but the contrast obtained on the "internal" side investigated by AFM is much weaker ($\approx$ 3 nm). This fact must be due to the complex phenomena involved in the microtome cutting operation.

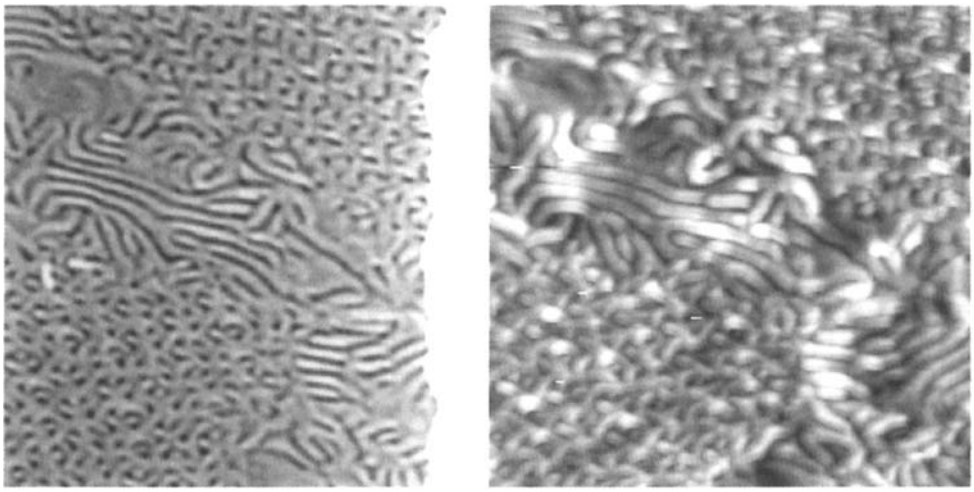

FIGURE 7 a) TEM image (negative); the white area on the right corresponds to the copper grid. b) AFM image of the same area. The size is 5 ×5 μm.

In conclusion, the contrast in the AFM and TEM images seems to be induced mainly by the topography of the external side of the cut.

The amplitude of the topography depends also on the thickness of the cut. Typically, when cuts a few hundred nm thick are investigated, neither the external nor the internal side exhibits significant topography contrast.

As mentioned in ref.(2,9), the observation of edge dislocations of distinct contrasts in the Ch* domains (λ^+ λ^- type is the most common as it has no core) allows the association of the dark regions of the TEM negative images with a director orientation perpendicular to the cut surface. In the case of the AFM images, the contrast obtained is consistent with this result: the thick regions appear in white and the thin ones in black, which gives rise to an identical situation. Both the TEM and AFM contrasts are therefore concordant when associating the crest regions of the relief to a bulk director parallel to the surface of the cut and the valley ones to a director normal to it.

NUMERICAL SIMULATIONS OF BLUE PHASE SECTIONS

Our aim was to compare from a qualitative point of view experimental AFM topographies with hypothetical topographies that can be generated within the frame of the theoretical Landau-de Gennes -like model of BPI elaborated by Grebel, Hornreich and Shtrikman[5].

We used the analytical expressions of the tensorial order parameter $Q_{ij}(\underline{r})$ derived by Grebel and al.[5] in the high chirality approximation where only twelve Fourier components with wave vectors disposed along the edges of a regular tetrahedron (these are [110] type vectors of the FCC reciprocal lattice of the BCC O[8] structure) are taken into account:

$$\begin{bmatrix} S_2 - 3S_2C_3 & \sqrt{2}(C_1C_3 + S_2S_3) - S_2C_1 & \sqrt{2}(C_3C_2 + S_1S_2) - S_1C_3 \\ \sqrt{2}(C_1C_3 + S_2S_3) - S_2C_1 & \Sigma_2 - 3S_3C_1 & \sqrt{2}(C_2C_1 + S_3S_1) - S_3C_2 \\ \sqrt{2}(C_3C_2 + S_1S_2) - S_1C_3 & \sqrt{2}(C_2C_1 + S_3S_1) - S_3C_2 & \Sigma_2 - 3S_1C_2 \end{bmatrix}$$

with $\Sigma_2 = S_1C_2+S_2C_3+S_3C_1$, $C_i = \cos(q_0\, x_i)$, $S_i = \sin(q_0\, x_i)$, $q_0=2\pi/a$, where a is the cell parameter of the cubic phase.

Using this model of BPI, we consider now a section defined by a plane having a normal $N(\theta, \phi)$ and situated at a distance h from the origin (Fig. 8.a). Let ξ and η be local cartesian coordinates in the plane of the section.

The topography resulting from the mean orientation of the molecules in the plane of the section depends on the preferential directions of the molecules and the degree of orientation around these directions at each point (ξ, η) of the plane. These preferential directions in the plane of the section are given by the eigenvectors $\hat{e}_i$ of $Q_{ij}(\xi, \eta)$ and the degrees of orientation by the eigenvalues $\lambda_i(\xi, \eta)$. If the eigenvalues are all different, the area is locally biaxial and if two of them are equal, it is uniaxial.

We visualise the spatial organisation of the molecules with rectangular boxes. They represent a convenient way to take into account both the preferential directions (the directors) and the degrees of order (biaxiality) (Fig. 8.b).

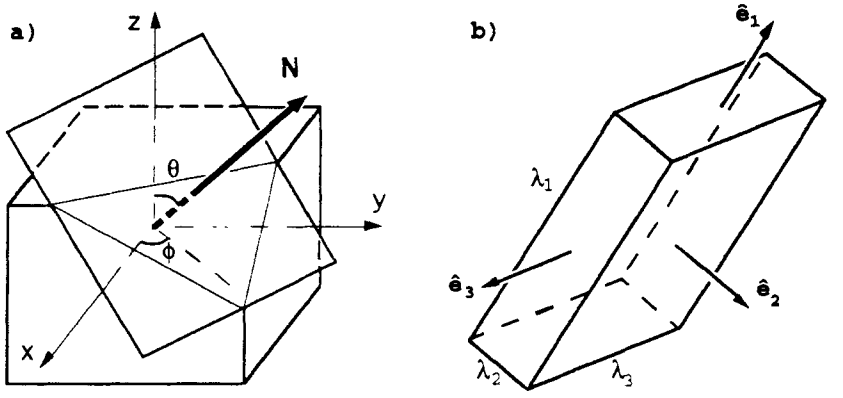

FIGURE 8 a)Section; b)Representation of the molecular organisation.

As a first step, we use the most simple algorithm to obtain a hypothetical topography: we choose to project the eigenvector (the local director) associated to the higher eigenvalue (uniaxial approximation) onto the normal N. This yields a low value if the director is into the plane of the section and a higher one if it is orthogonal to this plane.

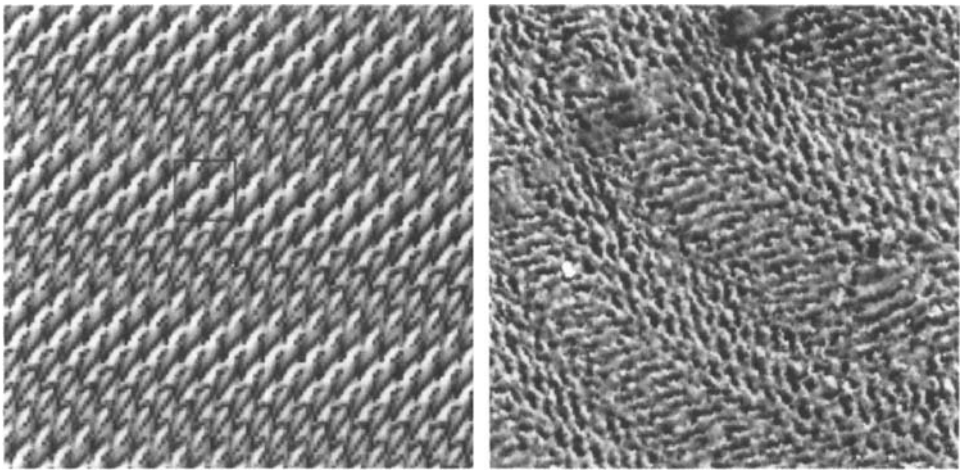

FIGURE 9 Numerical relief (left); AFM image (right).

We show on Fig. 9 an example of relatively good qualitative agreement between the experimental topography

observed in AFM experiments and a numerical one, obtained with $\theta = 0.335\ \pi, \phi = 0.35\ \pi$, $h = 10$ and $q_0 = 0.6$.

In Fig. 10, we visualise the director field with the rectangular box representation for a small area of the topography pattern shown in Fig. 9.

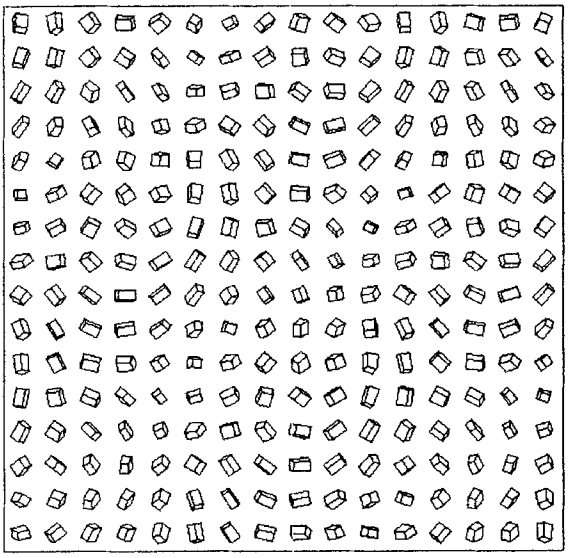

FIGURE 10 Director field in a small area from Fig.9.

In the future, we shall try to make more quantitative comparison of the diffraction patterns observed both experimentally (TEM, AFM) and numerically, in order to improve the algorithm used for the hypothetical surfaces.

DISCUSSION

These experiments rose new questions concerning the mechanism of cut-induced surface topography. In general, this mechanism must involve the orientation of the sample axes with respect to the orthonormal reference frame ($\underline{l}$, $\underline{n}$, $\underline{m}$) formed by the normal $\underline{n}$ to the average surface of the cut and by the normal $\underline{m}$ to the knife edge $\underline{l}$ and to $\underline{n}$. In the case of a cholesteric sample, this orientation is defined by the twist axis $\underline{t}$.

A possible process of the microtome cutting consists in the propagation of a crack along the direction $\underline{m}$, so that the model developed in ref. (7) could tentatively be used to explain the microtome induced topography[6]. This model predicts the disappearance of the corrugation and of the related TEM contrast when the helix axis is parallel either (1°) to $\underline{n}$ or (2°) to $\underline{m}$. The first prediction is consistent with the topography in the area labelled 1 of Fig. 6. Indeed, in this area the decrease in the amplitude of corrugation is correlated with an increase of its period, (the latter indicating that the helix axis $\underline{t}$ becomes parallel to $\underline{n}$). On the contrary, the second prediction is in contradiction with our experiments: in the area labelled 2 of Fig. 6, the amplitude does not depend on the orientation of the helix axis (here, the axis $\underline{t}$ remains orthogonal to $\underline{n}$, and rotates by $-\pi$ around the λ^- disclination) in the cholesteric fingerprint pattern, neither with TEM or with AFM techniques. We consider developing the model so that it can describe the observed topography.

Unlike the models developed in the frame of biological analogues of liquid crystals[8] (in this last case the fibrilar nature of the material involved can modify strongly the effects related to the cuts) we found an ample cut-induced corrugation of the surface only on the external surface of the thin cuts.

The conclusion we[2] and other authors[9] formerly reached on the association of the white and dark regions of the TEM photomicrograph respectively with the perpendicular and parallel orientation of the director relative to the cut surface, on the basis of the TEM observation of the non singular dislocations of the cholesteric lamellae, was largely questioned. Our recent AFM work confirms this previous conclusion. TEM contrast is related to the local orientation of the director. This was also strongly suggested by the observation of the [200] spots in the indexed diffraction pattern.

CONCLUSION

The complex phenomena involved in these cut mechanisms and the precise origin of the TEM contrast associated with cholesteric or BPI bulk structures remain unsettled questions. In the hypothesis of a TEM contrast directly related to the surface corrugations, the numerical simulations we initiated will give us the opportunity to compare the theoretical models on biaxial blue phase (Ginzburg-Landau approach), with our experimental situation. In particular, the Fourier transform of the numerical cuts, with simulated corrugations, will be compared with the experimental diffraction patterns.

ACKNOWLEDGEMENTS

We are grateful to Françoise Fried (Lab. Phys. Mat. Cond., Nice) and to Françoise Livolant (Lab. Phys. Sol., Orsay) for helpful discussions.

REFERENCES

1. J.M. Gilli, M. Kamayé and P. Sixou, J. Phys. France, 50, 2911 (1989).
2. J.M. Gilli, M. Kamayé and P. Sixou, Mol. Cryst. & Liq. Cryst., 199, 79 (1991).
3. H. Delacroix, J.M. Gilli, I. Erk, P. Mariani, Phys. Rev. Lett., 69, 2935 (1992).
4. M.A. Hallé, J.M. Gilli, P. Pieranski, Etude de la surface libre des cristaux liquides polymériques par la microscopie à force atomique, 6e Colloque d'Expression Française sur les Cristaux Liquides, September 1993, Chatenay-Malabry, France.
5. H.Grebel, R.M.Hornreich and S.Shtrikman, Phys. Rev. A, 28, 1114 (1983).
6. T. J. Bunning, D. L. Vezie, P. F. Lloyd, P. D. Haaland, E. L. Thomas, W. W. Adams, Liq. Cryst., 16, 769 (1994).
7. D. W. Berreman, S. Meiboom, J. A. Zasadzinski, M. J. Sammon, Phys. Rev. Lett., 57, 1737 (1986).
8. Y. Bouligand, Tissue & Cell, 4, 189 (1972), and related papers from the same author;
   M. M. Giraud-Guille, Tissue & Cell, 18, 603 (1986).
9. H. Hara, T. Satoh, T. Toya, S. Iida, S. Orii, J. Watanabe, Macromolecules, 21, 14 (1988).